International Journal of Signal Processing, Image Processing and Pattern Recognition
Vol. 8, No. 2 (2015), pp. 157-164
http://dx.doi.org/10.14257/ijsip.2015.8.2.16

Multi-Focus Image Fusion Based on Sparse Decomposition

Yongxin Zhang

School of Information Technology, Luoyang Normal University, Luoyang, 471022, China
tabo126@126.com

Abstract

In order to effectively improve fusion quality, a novel multi-focus image fusion approach with sparse decomposition is proposed. The source images are decomposed into principal and sparse components by robust principal component analysis (RPCA) decomposition. A sliding window technique is applied to inhibiting blocking artifacts. The focused pixels of the source images are detected by using the salient features within the sliding window and integrated to construct the final fused image. Experimental results show that the proposed scheme can significantly inhibit the blocking artifacts compared to the other existing fusion methods in terms of some visual and objective evaluations.

Keywords: *image fusion, robust principal component analysis, sliding window, sparse feature*

1. Introduction

Image fusion can be defined a process in which a single sharper image is produced by integrating a set of source images captured from the same scene with different focus points [1]. The traditional image fusion methods can be categorized into two groups: spatial domain fusion and transform domain fusion [2]. This paper particularly focuses on the spatial domain methods. Image fusion can be defined as a process in which a single sharper image is produced by integrating a set of source images captured from the same scene with different focus points [1]. The traditional image fusion methods can be categorized into two groups: spatial domain fusion and transform domain fusion [2]. The spatial domain fusion methods partition the source images into blocks or regions by using their region homogeneity, and detect the focused blocks or regions by using their local spatial features [3], such as energy of image gradient (EOG) [4] and spatial frequency (SF) [5]. Then, the focused blocks or regions are integrated to construct final fused image. The spatial domain methods are easy to implement and have low time consumption [1]. However, the blocking artifacts may compromise the quality of the final fused image. For eliminating the blocking artifacts, researchers have developed many improved schemes. Y. Zhang, *et al.*, [6] have selected the best focus by using non-negative matrix factorization and improved the visual quality of the fused image. Aslantas, *et al.*, [7] have selected the optimal block-size by using differential evolution algorithm and enhanced the self-adaptation of the fusion method. But this method requires longer computational time. Wu, *et al.*, [8] have selected the focused patches from the source images by using a belief propagation algorithm. But the algorithm is complicated and time-consuming. Y. Zhang, *et al.*, [9] have detected the focused blocks by using pulse coupled neural network. The iterative procedure is time-consuming. De, *et al.*, [10] have determined the optimal block-size by using quad tree structure and effectively solved the problem of determining of block-size. These schemes all achieve better performance than the traditional methods and significantly inhibit the blocking artifacts. But they cannot eliminate the blocking artifacts completely.

ISSN: 2005-4254 IJSIP

In this paper, a novel image fusion scheme different from the methods mentioned above is proposed. This method is implemented in the robust principal component analysis (RPCA) decomposition domain. RPCA is a very important method for low-rank matrix recovery (LRMR) [11]. Wan, *et al.*, [12] have investigated the potential application of RPCA in image fusion and achieved a consistently good fusion result. However, their method requires longer computational time for the application of sliding window techniques. Candes, *et al.*, [11] have extended the RPCA to the background modelling from surveillance video. They correctly identified the moving pedestrians in the foreground by using the sparse component of surveillance video. The sparse component effectively represents the salient feature of the foreground objects. As is known, the focused objects in the foreground are very important for multi-focus image fusion. Motivated by Candes's idea, this paper tries to establish a multi-focus image fusion scheme using RPCA decomposition. Different from Wan's method, the main contribution of this paper is that a new method based on sparse decomposition is proposed for image fusion. The sparse components of the source images are obtained by using RPCA decomposition. The focused pixels are detected by computing the salient feature of the corresponding sparse component. The proposed method can significantly inhibit the blocking artifacts and better extract the focused image details from the source images.

The rest of the paper is organized as follows. In Section 2, the new method based on RPCA decomposition for image fusion is proposed. In Section 3, extensive simulations are performed to evaluate the performance of the proposed method. In addition, several experimental results are presented and discussed. Finally, concluding remarks are drawn in Section 4.

2. Proposed Method

According to the advantages of RPCA, we try to establish a scheme to improve the accuracy of the focused regions detection while inhibit the blocking artifacts of the fused image. The proposed fusion framework is depicted in Figure 1.

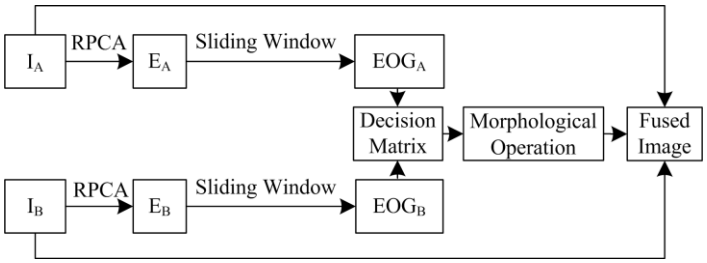

Figure 1. Block Diagram of Proposed Multi-Focus Images Fusion Framework

For simplicity, this paper assumes that there are only two source images, namely I_A and I_B, respectively. The rationale behind the proposed scheme applies to the fusion of more than two multi-focus images. The source images are assumed to pre-registered and the image registration is not included in the framework.

2.1. Fusion Algorithm

The fusion algorithm consists of the following three steps:

Step 1: Construct the data matrix. The source images $\{I_A, I_B\}, I_A, I_B \in ¡^{M \times N}$ are converted into column vectors $I_A^c, I_B^c \in ¡^{MN \times 1}$, respectively. Thus, data matrix D is defined as:

$$D = [I_A^c; I_B^c] \quad (1)$$

Step 2: RPCA decomposition is performed on D to obtain a principal matrix $A \in ¡^{2MN \times 1}$ and a sparse matrix $E \in ¡^{2MN \times 1}$, respectively. The sparse matrix $E \in ¡^{2MN \times 1}$ is computed through inexact augmented Lagrange multipliers algorithm (IALM) of RPCA [11], which is an version implementation for recovering low-rank matrices and has been reported to yield similar results with much less time consumption. The sparse matrix $E \in ¡^{2MN \times 1}$ is then converted into matrices $E_A, E_B \in ¡^{M \times N}$ corresponding to the source images I_A and I_B, respectively.

Step 3: According to the fusion rules, focused pixels belonging to the focused regions are integrated to obtain the fused image.

2.2. Fusion Rule

There are two key issues [2] involved with the fusion rules. The first is how to measure the activity level of the source images, which recognizes the sharpness of the source images. Figure 2 shows the multi-focus images 'Disk' and their different components. Figure 2 (a) shows the multi-focus source images 'Disk'. Figures 2 (b-c) show the corresponding images of the principal components and sparse components, respectively. It is obvious that the salient features of sparse matrix agree well with the local features of the sharper objects in source images. Thus, the focused regions can be detected by comparing the salient features computed from the sparse matrix. We use the EOG of the pixels within a $M \times N$ ($\mathrm{M} = 2s+1, N = 2t+1$) window of the sparse components to measure the activity level, respectively. s and t are all positive integers. The EOG is calculated as:

$$\begin{cases} EOG(i,j) = \sum_{m=-(M-1)/2}^{(M-1)/2} \sum_{n=-(N-1)/2}^{(N-1)/2} (I_{i+m}^2 + I_{j+n}^2) \\ I_{i+m} = I(i+m+1, j) - I(i+m, j) \\ I_{j+n} = I(i, j+n+1) - I(i, j+n) \end{cases} \tag{2}$$

where $I(i,j)$ indicates the value of the pixel location (i,j) in the source images. The size of the window is set as 5×5.

The other is how to integrate the focused pixels or regions from the source images into the counterparts of the fused image. In order to eliminate the blocking artifacts, a sliding window technique is applied to the sparse components, respectively. Let $EOG_{(i,j)}^{E_A}$ and $EOG_{(i,j)}^{E_B}$ denote the EOG of all the pixels within the sliding windows which cover the neighborhood region of the pixel location (i,j) in E_A and E_B, respectively. The EOG of the neighborhood region of the pixel location (i,j) in E_A and E_B are respectively compared to determine which pixel is likely to belong to the focused regions. A decision matrix H is constructed for recording the comparison results as follows:

$$H(i,j) = \begin{cases} 1, & EOG_{(i,j)}^{E_A} \geq EOG_{(i,j)}^{E_B} \\ 0, & otherwise \end{cases} \tag{3}$$

where "1" in H indicates the pixel location (i,j) in image I_A is in focus while "0" in H indicates the pixel location (i,j) in image I_B is in focus. However, judging by EOG alone is not sufficient to distinguish all the focused pixels. There are thin protrusions, narrow breaks, thin gulfs, small holes, *etc.*, in H. To overcome these disadvantages, morphological operations [6] are performed on H. Opening, denoted as $H \circ Z$, is simply erosion of H by the structure element Z, followed by dilation of the result by Z. This process can remove thin gulfs and thin protrusions. Closing, denoted as $H \bullet Z$, is

dilation, followed by erosion. It can join narrow breaks and thin gulfs. To correctly judge the small holes, a threshold is set to remove the holes smaller than the threshold. Thus, the final fused image is constructed as follows:

$$F(i,j)=\begin{cases} I_A(i,j) & H(i,j)=1 \\ I_B(i,j) & H(i,j)=0 \end{cases} \quad (4)$$

where $I_A(i,j)$ and $I_B(i,j)$ denote the values of the pixels at position (i,j) in the source images I_A and I_B, respectively.

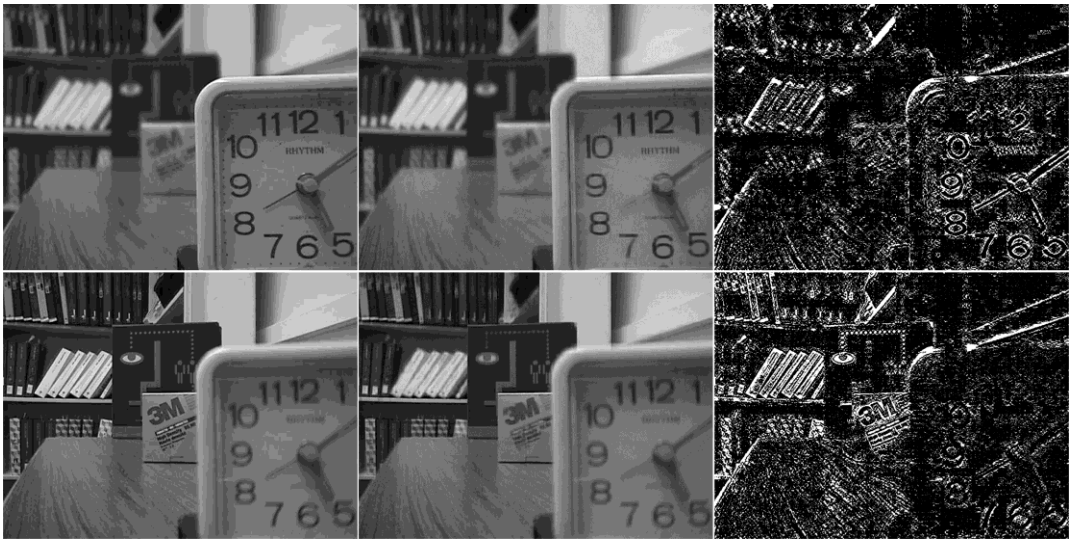

(a) (b) (c)

Figure 2. Decomposition of Multi-Focus Images 'Disk' using RPCA (a) source Images, (b) Principal Components, (c) Sparse Components

3. Experimental Results

In order to evaluate the validity of the proposed method, the experiment is performed on a set of 2 pairs of multi-focus source images [13] differing in content and texture, as are shown in Figure 3. The two pairs are grayscale images with size of 640×480 pixels and 512×384 pixels, respectively. In this paper, all the source images are assumed to have been registered. Experiments are conducted with Matlab in Windows environment on a computer with Intel core(TM) i7-4770 and 4G memory. For comparison, beside the proposed method, some existing multi-focus image fusion methods are also implemented on the same set of source images. These existing methods include discrete wavelet transform (DWT), nonsubsumpled contourlet transform (NSCT), SF, principal component analysis (PCA), RPCA (Wan's method [12]). Due to the lack of original source code, the Eduardo Fernandez Canga's Matlab image fusion toolbox [14] is used as the reference for DWT, SF and PCA. Specifically, the Daubechies wavelet function 'bi97' is used in the DWT. The decomposition level of DWT is 4. The NSCT toolbox [15] is used as the reference for NSCT. The RPCA toolbox [16] is used as the reference for RPCA decomposition. The pyramid filter '9-7' and the orientation filter '7-9' with {4, 4, 3} levels of decomposition are set for the fusion method based on NSCT. The sliding window size in RPCA is 35×35. In order to quantitatively compare the performance of the proposed method and that of the others mentioned above, two metrics are used to evaluate the fusion performance. They are: (i) Mutual information (MI) [17], which measures the degree of dependence of the source image and the fused image. (ii) $Q^{AB/F}$ [18], which reflects the amount of edge information transferred from the source images to the fused image. In these methods, a larger value signifies a better fusion result.

(a) (b) (c) (d)

Figure 3. Multi-Focus Source Images (a) Near Focused Image 'Rose', (b) far Focused Image 'Rose', (c) Near Focused Image 'Book', (d) Far Focused Image 'Book'

For qualitative comparison, the fused images 'Rose' and 'Book' obtained by different methods are shown in Figures 4 (a-f) and Figures 5 (a-f). The difference images between the far focused source image 'Book' and corresponding fused images obtained by different methods are shown in Figures 6 (a-f).

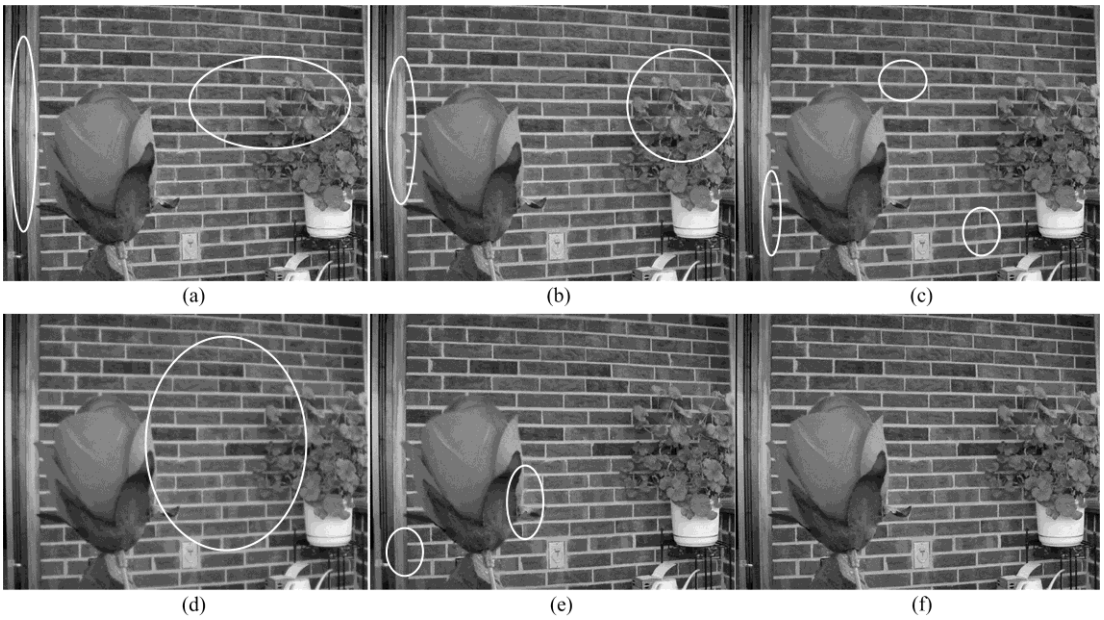

(a) (b) (c)

(d) (e) (f)

Figure 4. Fused Images 'Rose' Obtained by DWT (a), NSCT (b), SF (c), PCA (d), RPCA (e) and the Proposed Method (f)

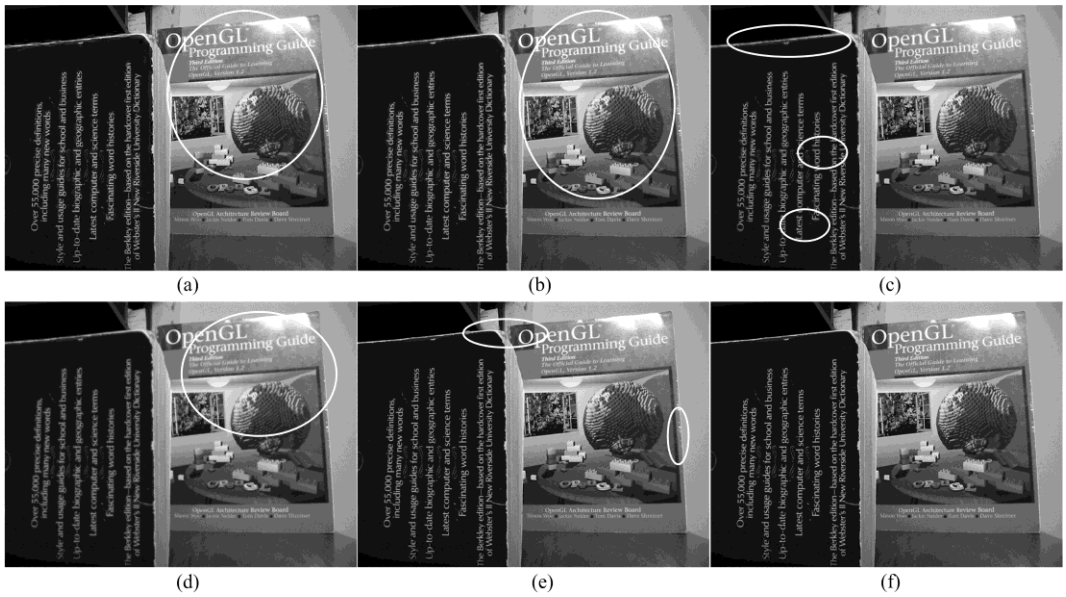

Figure 5. Fused Images 'Book' Obtained by DWT (a), NSCT (b), SF (c), PCA (d), RPCA (e) and the Proposed Method (f)

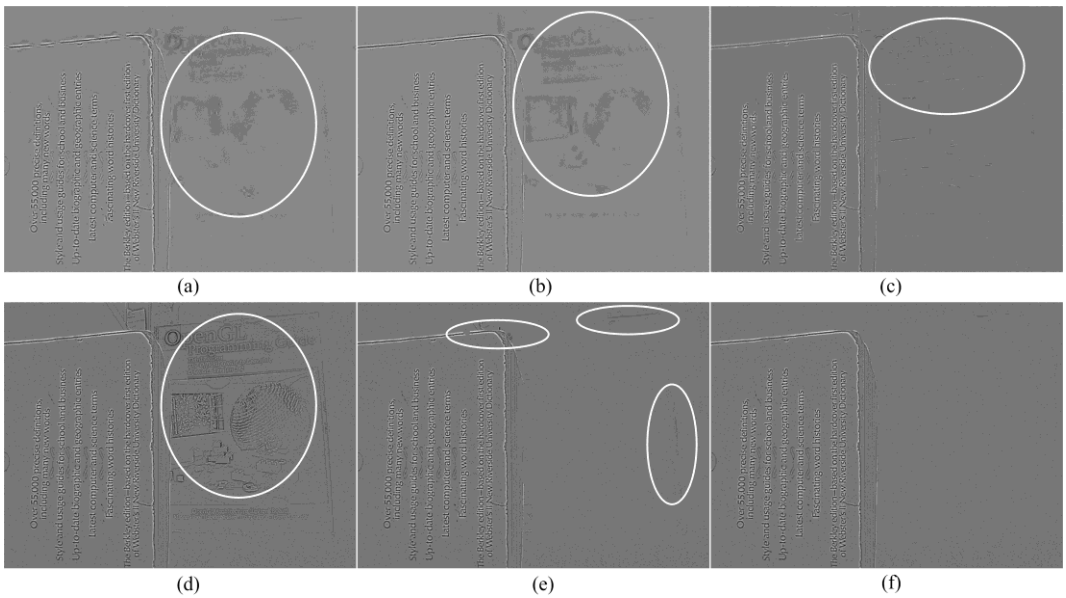

Figure 6. Difference Images Between Source Image 'Book' far Focused and Corresponding Fused Images Obtained by DWT (a), NSCT (b), SF (c), PCA (d), RPCA (e) and the Proposed Method (f)

The fused images obtained by DWT and NSCT demonstrate obvious blur, such as the upper edge of the plant in Figures 4 (a-b) and the cover of the right book in Figures 5 (a-b). The obvious blocking artifacts appear in the fused image obtained by SF, such as the left door frame in Figure 4(c) and the cover of the left book in Figure 5 (c). The low contrast appears in the fused image obtained by PCA, such as Figures 4 (d) and 5 (d). The blocking artifacts also appear in the fused images obtained by RPCA, such as the right edge of the rose in Figure 4 (e) and edge of the book in Figure 5 (e). The obvious mis-registration and distortion appear in Figures 6 (a-b). The obvious residual can be seen in the right region of Figure 6 (e). The edge and details in Figures 4 (f) and 5 (f) are clear. The right region of Figure 6 (f) is smooth and complete. It is easy to see that the visual

quality of the fused images obtained by the proposed method is better than that of the fused images obtained by the other methods.

For quantitative comparison, the quantitative results in two quality measures are shown in Table 1. The running times of different methods are also shown in the Table. The proposed method gains higher MI and $Q^{AB/F}$ values than the other methods. The running time of Wan's method is obviously larger than that of the proposed method. Due to the matrix decomposition accounts for the majority of the computational load, the proposed method still yields larger computational cost than DWT-based method, SF-based method and PCA-based method.

Table 1. Performance of Different Fusion Methods

Method	Book			Rose		
	MI	$Q^{AB/F}$	**Run-time(s)**	**MI**	$Q^{AB/F}$	**Run-time(s)**
DWT	6.82	0.69	0.56	4.78	0.67	0.18
NSCT	7.33	0.72	74.18	5.19	0.70	47.44
SF	8.41	0.70	0.48	6.78	0.71	0.30
PCA	7.74	0.63	0.18	5.45	0.71	0.01
RPCA	9.28	0.72	21.46	7.98	0.71	13.84
Proposed	**9.33**	**0.73**	5.55	**8.18**	**0.72**	4.33

4. Conclusion and Future work

This paper proposes a novel multi-focus image fusion method using sparse decomposition to improve the fusion quality. The performance evaluations have demonstrated that the proposed method can produce better fused image and significantly inhibit the blocking artifacts. However, the proposed method has high computational cost for the matrix decomposition. In the future, we will consider optimizing the proposed method to reduce the computational cost.

Acknowledgements

The work is supported by the National Key Technology Science and Technique Support Program (No. 2013BAH49F03), the National Nature Science Foundation of China (No. 61379010), the Key Technologies R&D Program of Henan Province (No. 142102210637).

References

[1]. H. Hariharan, "Extending Depth of Field via Multi-focus Fusion", PhD Thesis, the University of Tennessee, Knoxville, **(2011)**.
[2]. Y. Zhang, L. Chen, Z. Zhao and J. Jia, "Multi-focus Image Fusion Based on Non-negative Matrix Factorization and difference images", Signal Processing, vol. 105, **(2014)**.
[3]. W. Huang and Z. Jing, "Evaluation of focus measures in multi-focus image fusion", Pattern Recognition Letters, vol. 28, no. 9, **(2007)**.
[4]. A. M. Eskicioglu and P. S. Fisher, "Image quality measures and their performance", IEEE Trans. Communication, vol. 43, no. 12, **(1995)**.
[5]. S. Li, J. Kwok and Y. Wang, "Multifocus image fusion using artificial neural networks", Pattern Recognition Letters, vol. 23, no. 8, **(2002)**.
[6]. Y. Zhang, L. Chen, Z. Zhao and J. Jia, "A Novel Multi-focus Image Fusion Method Based on Non-negative Matrix Factorization", TELKOMNIKA Telecommunication, Computing, Electronics and Control, vol. 12, no. 2, **(2014)**.
[7]. V. Aslantas and R. Kurban, "Fusion of multi-focus images using differential evolution algorithm", Expert System with Application, vol. 37, no. 12, **(2010)**.
[8]. W. Wu, X. M. Yang, Y. P. J. Pang and G. Jeon, "A multifocus image fusion method by using hidden Markov model", Opt. Communication, vol. 287, **(2013)**.

[9]. Y. Zhang, L. Chen, Z. Zhao and J. Jia, "A Novel Pulse Coupled Neural Network Based Method for Multi-focus Image Fusion", International Journal of Signal Processing, Image Processing and Pattern Recognition. vol. 7, no. 3, **(2014)**.
[10]. I. De and B. Chanda, "Multi-focus image fusion using a morphology-based focus measure in a quad-tree structure", Information Fusion, vol. 14, no. 2, **(2013)**.
[11]. E. Candes, X. Li, Y. Ma and J. Wright, "Robust principal component analysis?", JACM, vol. 58, no. 3, **(2011)**.
[12]. T. Wan, C. Zhub and Z. Qin, "Multifocus Image Fusion Based on Robust Principal Component Analysis", Pattern Recognition Letters, vol. 34, no. 9, **(2013)**.
[13]. http://www.ece.lehigh.edu/spcrl, online image database, Accessed **(2013)** April 17.
[14]. http://www.imagefusion.org/, Image fusion toolbox, Accessed **(2013)** March 20.
[15]. http://www.ifp.illinois.edu/minhdo/software/, NSCT toolbox, Accessed **(2013)** January 20.
[16]. http://perception.csl.illinois.edu/matrix-rank/sample_code.html, RPCA toolbox, Accessed **(2013)** January 10.
[17]. D. J. C. MacKay, "Information theory, inference and learning algorithms", Cambridge university press, **(2003)**.
[18]. C. S. Xydeas and V. Petrovic, "Objective image fusion performance measure", Electronics Letters, vol. 36, no. 4, **(2000)**.

Authors

Yongxin Zhang is a PhD working at the School of Information Technology, Luoyang Normal University, Luoyang, China. His research interests include image processing and pattern recognition.

